Experimental Investigation of Dapped Ends with Diagonal Reinforcement

Peer-reviewed author version

Rajapakse, Chathura; DEGEE, Herve & Mihaylov, Boyan (2024) Experimental Investigation of Dapped Ends with Diagonal Reinforcement. In: ACI STRUCTURAL JOURNAL, 121 (4) , p. 35 -46.

DOI: 10.14359/51740710
Handle: http://hdl.handle.net/1942/43492

EXPERIMENTAL INVESTIGATION OF DAPPED ENDS WITH DIAGONAL REINFORCEMENT

by Chathura Rajapakse, Hervé Degée and Boyan Mihaylov

Biography: Chathura Rajapakse is a Senior Lecturer at Department of Civil Engineering, University of Moratuwa, Sri Lanka. He completed his PhD at University of Liège and Hasselt University, Belgium in 2023. He received his BSc Eng. and MPhil from University of Peradeniya, Sri Lanka in 2015 and 2018, respectively. His research interests include kinematics-based modelling and nonlinear finite element analysis of concrete structures.

Hervé Degée is Professor of Structural Design at Hasselt University (Belgium), where he is heading the Structural Testing Laboratory. His research activities cover a rather broad range of structural aspects, with a main focus on bridges, unconventional steel-concrete structural solutions and seismic resistance of steel and masonry structures. He is also very active in the development of European standards for structural design.

Boyan Mihaylov is an Associate Professor of Civil Engineering at University of Liege, Belgium. He completed his PhD at University of Pavia, Italy in 2009 and was Postdoctoral Fellow at University of Toronto until 2013. His research interests include the development of his macro-kinematic approaches for the behavior of disturbed concrete regions and members, as well as the assessment and retrofit of existing concrete structures.

ABSTRACT

Reinforced concrete dapped-end connections are susceptible to formation of inclined cracks at the re-entrant corner under service conditions. As these connections also work with high shear stresses, they require a high amount of reinforcement to ensure sufficient load-bearing capacity. To deepen the understanding of this topic, an experimental campaign of eight large-scale

dapped-end connections featuring diagonal reinforcement is presented. These specimens, which are among the largest available in the literature, are similar in size to dapped ends typically used in bridges. The test series captures both flexural and shear failures of dapped ends. The crack displacements, crack patterns and elongation of main reinforcement are reported with 56 continuous measurements of deformations. The test results of this study are used in conjunction with a similar study on specimens with orthogonal reinforcement to investigate the impact of reinforcement layout. For the same amount of dapped-end reinforcement, specimens with diagonal reinforcement are considerably stronger than the corresponding connections with orthogonal reinforcement. For both reinforcement layouts, the crack widths exceeded typical code provisions under service conditions.

Keywords: dapped-end connections, diagonal reinforcement layout, re-entrant corner cracks, flexural failures, shear failures

INTRODUCTION

Dapped-end connections, also known as half-joints, feature a sudden reduction of cross-sectional depth at a sharp re-entrant corner (Fig. 1). This characteristic shape offers convenient and simple connection of precast structural elements, while allowing to maintain a constant construction depth. As a consequence, these connections are commonly used in reinforced and prestressed concrete structures of bridges, parking garages, industrial buildings, and other precast infrastructure. While the shape of the connection provides certain advantages, it also results in the concentration of stresses at the re-entrant corner. These stresses exceed the tensile strength of the concrete under service loads and restrained shrinkage, leading to the formation of inclined corner cracks. Excessive opening of such cracks raises major durability concerns in bridges, as these connections are typically located at expansion joints in the superstructure, where penetration of water and deicing salts may occur. In order to control these cracks and

ensure sufficient load-bearing capacity of the connection, it is often necessary to provide dense horizontal, vertical and/or diagonal reinforcement in the vicinity of the re-entrant corner. Therefore, efficient use of reinforcement and the choice of reinforcement layout in the dapped ends becomes an important design and practical consideration.

Dapped-end connections typically feature two main reinforcement arrangements, which are often referred to as the orthogonal layout and the diagonal layout. The orthogonal layout consists of longitudinal reinforcement at the bottom of the dapped end and stirrups in the full-depth section. The second approach combines the orthogonal reinforcement with the provision of inclined (diagonal) reinforcement that intersects the corner crack at the perpendicular direction. Desnerck et al. 2016[1] report that the orthogonal layout is more common in the United States while the diagonal layout is often used in Europe. The two reinforcement layouts correspond to different flow of forces in the dapped end, which is typically visualized using strut-and-tie models[2-5] (STM) or stress fields[6-7] – see Fig. 1. These models feature main horizontal, vertical, and diagonal ties at the re-entrant corner (reinforcement in tension), as well as inclined struts in the dapped end (concrete in compression). Figure 1 shows a common STM for the diagonal reinforcement layout, where a portion of the load is transferred through the orthogonal layout and the rest via diagonal bars (ties).

The influence of reinforcement layout on the behavior of dapped-end connections has been a topic of significant research interest due to its practical importance. Several past experimental studies have been performed on dapped-end specimens featuring different geometrical and material properties[1, 4-5, 7-18]. However, while many of the past studies provide important information on the failure mode and strength of dapped-end connections, there remains a need for tests with continuous measurements of important deformations, including crack kinematics. Furthermore, the greater majority of tests from the literature are laboratory-scale specimens, where the depth of the dapped end is in the range of 100 mm to 350 mm. As connections in

existing structures are typically much larger, there is a need for similarly large-scale test specimens that are more representative of the construction practice. To address these concerns, an experimental campaign was conducted and reported by the authors, which featured eight large-scale dapped-end tests with extensive instrumentation of the connections[19]. The specimens had an orthogonal reinforcement layout, a full depth of 1000 mm, and a depth of the dapped end of 500 mm (half joint).

In this paper, a similar experimental study on dapped-end connections with diagonal reinforcement layout is presented. Detailed measurements of crack patterns, crack widths, reinforcement and concrete strains are reported in conjunction with a comprehensive description of the behavior of test specimens. The test results from this study are compared to those from the previous study on orthogonal reinforcement[19] to investigate the effect of reinforcement layout.

RESEARCH SIGNIFICANCE

This paper presents experimental research on eight dapped-end connections, which are among the largest in the literature. Complete behavior of the test specimens at both service and ultimate conditions is provided with the aid of extensive continuous measurements of deformations. Hence these tests, which feature the main failure modes of dapped-end connections, contribute to the state-of-the-art with an in-depth description and analysis of specimens that are representative of existing connections. The analyses and comparisons performed in this study provide quantitative information on strength, ductility, and crack control of dapped-end connections with diagonal and orthogonal reinforcement layouts.

EXPERIMENTAL PROGRAM

The experimental program features eight large-scale dapped-end connections with the diagonal reinforcement layout. The tests aim to capture both flexural and shear failures observed in such connections, and further investigate them using detailed deformation measurements.

Another objective of the experimental program was to allow for direct and fair comparisons between the specimens with diagonal reinforcement layout of this study (DL series) and the specimens with orthogonal layout (OL series) from the previous study conducted by the authors[19]. Therefore, it was decided to have identical geometry of the specimens, identical test setup and loading protocols, as well as similar material properties as in the previous study. While essential information about the test specimens with orthogonal layout is provided briefly in this paper, the reader is directed to the original publication[19] for a complete description. In this section, an in-depth description of the experimental program pertaining to the current study is presented.

Test specimens

Figure 2 shows the geometry and reinforcement details of the test specimens featuring the diagonal reinforcement layout. Four beams were cast, where each beam had two dapped-end connections, providing eight test specimens in total. The cross-sectional dimensions of the dapped ends were 500×350 mm, while the full-depth portion of the beams had a 1000×350 mm section. The main horizontal reinforcement was provided in the form of hairpin bars to ensure adequate anchorage at the end of the dapped end, while the transverse reinforcement comprised closed stirrups with 90° hooks arranged in either two-legged or four-legged layers. The bottom reinforcement of the beam section included straight bars extending along the entire length between the dapped ends, as well as short bars at both ends. The short bars were lap-spliced with the long bars and were anchored via 100×50×25 mm welded steel plates.

Table 1 summarizes the main test variables of this study (DL series) and also provides

information from the previous OL series for completeness. The amounts of horizontal and vertical reinforcement in the DL series were selected to be approximately one-half of that in the OL series. The diagonal reinforcement of the DL series was determined to ensure approximately equal contributions of the two load paths shown in Figure 1 (i.e. $V = V_1 + V_2$ where $V_1 \approx V_2$). Within each beam from the DL series, the two dapped ends had identical amounts of horizontal and diagonal reinforcement near the re-entrant corner, but different amounts of vertical reinforcement. The ratio between the area of horizontal and vertical reinforcement was either A_{sh}/A_{sv}≈1.50 or ≈0.75. The reinforcement amount and diameters were gradually increased in the four beams, to capture a spectrum of flexural failures in the lightly reinforced specimens to shear failures in the more densely reinforced connections. The clear shear span of the dapped ends was not provided with vertical reinforcement (stirrups) to simulate the case of minimum shear resistance. Sufficient flexural and shear reinforcement was provided in the beam region between the dapped ends to ensure that the failures occurred in the end connections. Table 1 also lists the compressive strength of the concrete f_c which varied between 46.2 and 52.1 MPa, similar to f_c in the OL series. The reported values represent the average strength of three 150×300 mm cylinders tested on the day of the corresponding dapped-end test. The age of the specimens at the time of testing was approximately 10 months. The maximum size of coarse aggregates in the concrete was 16 mm.

The mechanical properties of the reinforcement used in the tests are reported in Table 2. Conventional European reinforcing bars, with a characteristic yield stress of 500 MPa and ductility class B according to EN 1992-1-1[20], were used in the specimens.

Test setup and instrumentation

The test setup used for the experimental campaign is presented in Figure 3. The beams were subjected to three-point bending such that only one of the two dapped-ends was tested at a time.

The testing dapped end rested on a roller support and a 200×500×50 mm steel plate. The other roller support was placed sufficiently far from the non-testing dapped end to avoid damage at that end. The load was applied on the top face of the beam with a 5 MN hydraulic jack equipped with a load cell and a hinge (pin). The distance between the load application point and the centers of the two supports was 1750 mm. The shear-span-to-effective-depth ratio of the dapped-end was 320mm/460mm=0.70, which is identical to the OL series. After testing the first dapped-end connection, the beam was turned to test the other end.

The instrumentation of the testing dapped end consisted of a series of displacement transducers (DT) and strain gauges – see Figure 3. The displacement transducers were mounted on the surface of the specimens at strategic locations to provide continuous measurements of both local and global deformations of the connections. DT 1 and 2 were placed along the main horizontal and vertical reinforcement near the re-entrant corner, while DT 5, 6 and 7 were arranged in a triangle to provide a global measure of the deformations in the connection. The horizontal and vertical components of the corner crack displacement were measured by DT3 and DT4, respectively. DT 1-7 were applied to one side face of each connection. The compressive deformations of the top concrete fibers were measured by DT 8-14, which were arranged in a chain on the top face of the beam.

The main dapped-end reinforcement was also instrumented with strain gauges to capture local tensile deformations. Two strain gauges were glued on the horizontal reinforcement (hairpin bars), two on the first layer of vertical reinforcement (stirrup legs), and two on the diagonal reinforcement. All six gauges were placed near the re-entrant corner of the connection where the corner crack was expected to intersect the reinforcement.

The beam was loaded in pressure-control until failure, typically in six load steps. The load was applied by manually increasing the pressure of the hydraulic jack. Initially the applied load was increased at a rate of approximately 20 kN/minute. Near failure this was done very slowly,

taking care not to increase the pressure if the load drops. At the end of each load step the loading was paused, crack patterns were photographed, and crack widths at selected locations were measured with crack comparators.

BEHAVIOR OF TEST SPECIMENS

The complete behavior of the eight test specimens from the DL series is discussed and compared with the help of Table 3 and Figure 4. Table 3 provides a series of important measurements taken at 50% of the peak load, at first yielding of the main dapped-end reinforcement, and at peak load (strength) of the connection. Corresponding results from the OL series are also provided (see shaded portion of the table), as reported elsewhere[19]. Figure 4 provides a detailed graphical overview of the DL series, which combines crack diagrams near peak load (left), photos after failure (middle) and load-deformation plots (right). The crack diagrams contain the strains along the top concrete surface (blue bars), and the average strains measured along the main horizontal, vertical, and diagonal dapped-end reinforcement (green bars). The load-deformation plots provide both local and global deformation measurements. DT3 (black curves) and DT 4 (blue curves) measurements show the horizontal and vertical displacement components of the inclined crack at the re-entrant corner. The global diagonal elongation of the dapped-end connection is provided by DT 7 measurements (red curves). Displacement DT2 minus DT4 (green curves) shows the sum of the vertical displacements of cracks intersecting DT2, excluding that of the main re-entrant corner crack.

In all eight tests of the DL series, first cracking occurred at the re-entrant corner, as typical for dapped-end connections. Table 3 shows that the support shear load at first cracking varied between 20 kN and 53 kN. Although subjected to some scatter, the general trend is that first cracking occurred at relatively higher support shear loads in the more lightly reinforced specimens (40 kN and 44 kN in 1-DL1 and 1-DL2). Despite having similar concrete strengths,

heavily reinforced specimens such as 4-DL7 and 4-DL8 displayed first cracking at relatively smaller support shear loads (16 kN and 24 kN). This reduction of first cracking load may have arisen due to restrained shrinkage strains. The observed trend is consistent with the increase of reinforcement amount in the DL specimens, as high amounts of reinforcement results in larger restrained shrinkage and consequently a smaller cracking load. A similar trend was observed in the test specimens from the OL series.

The re-entrant corner crack opened and propagated as the applied load was increased. At 50% of the peak resistance of the DL specimens, the horizontal crack displacements w_h reached values between 0.38 mm and 0.96 mm, while the vertical displacements w_v were between 0.35 mm and 0.93 mm. First yielding, which was identified based on the strain gauge readings without correcting for shrinkage strains, occurred in either the main vertical dapped-end reinforcement or in the diagonal reinforcement at load levels varying between 62% and 75% of the peak resistance. Except in the case of the most lightly reinforced specimen 1-DL1, the main horizontal reinforcement yielded last. This sequence of yielding is influenced by the bar diameters and the relative magnitudes of crack displacements. Although the diagonal reinforcement had relatively larger bar diameters, it also experienced bigger crack displacements due to its orientation, and hence in certain cases yielded first. For the stirrups, the faster yielding occurred due to their small bar diameters, which typically engage faster. The horizontal and vertical crack displacements at the re-entrant corner varied between 0.42 mm and 1.26 mm at first yielding. It is important to note that in the eight test specimens, all the main dapped-end reinforcement yielded prior to the failure of the connection. A similar trend was reported in the OL test series[19].

The measured strengths of the DL series in Table 3 show that, as the total amount of dapped-end reinforcement (A_{sh}+A_{sv}+A_{sd}) was increased approximately 5-fold from 697 mm^2 in specimen 1-DL1 to 3133 mm^2 in specimen 4-DL7, the strength of the connections increased

approximately 4-fold from 257 kN to 903 kN. This disproportionality is largely due to the change of failure mode observed in the test specimens. The lightly reinforced specimens such as 1-DL1 and 1-DL2 failed along a dominant re-entrant corner crack. As the reinforcement amount was increased, the corner crack was comparatively smaller at ultimate conditions, and the failure mode shifted to shear failures along inclined cracks in the dapped-end region. Consequently, the ductility of the heavily reinforced connections was reduced, in contrast to the lightly reinforced specimens. This global trend is illustrated in Figure 5, where the variations of support shear load with the diagonal elongation (DT7) are plotted. It can also be seen that, of the two dapped ends of each beam, the more heavily reinforced connection (dotted lines) generally showed slightly less ductility.

Figures 4a (left) and 4b (left) show the crack patterns near peak resistance of the most lightly reinforced specimens, 1-DL1 and 1-DL2. In both cases the re-entrant corner crack, which propagated nearly to the top of the beam, exhibited large displacements in excess of 6 mm prior to failure. It can be seen from the load-deformation plots in Figures 4a (right) and 4b (right) that the connections entered a long flexural plateau upon yielding of the main dapped-end reinforcement. The green bars shown in the crack patterns indicate that the average strains of the main dapped end reinforcement were well in excess of the yield strains. The compressive strains of the top longitudinal concrete fiber (blue blocks) were highest above the tip of the corner crack, with values in excess of -2×10^{-3}. At this high compressive strain, small horizontal cracks were observed in the concrete, indicating crushing of the material and the formation of a compression damage zone. The variation of compressive strains along the top face was symmetrical in nature and decayed close to zero on either side of the tip of the corner crack.

Figures 4c and 4d show the crack patterns and load-deformation plots of specimens 2-DL3 and 2-DL4, which had higher amounts of dapped-end reinforcement than the two connections of beam 1, 1-DL1 and 1-DL2. As the reinforcement amount was increased, there occurred several

secondary cracks parallel to the re-entrant corner crack. Near failure, the corner crack and the parallel crack propagating from the inner edge of the support were the widest, with the corner crack reaching displacements in excess of 4 mm. Eventually, the main vertical reinforcement ruptured in the wide cracks, causing the failure of the connections. The splitting cracks along the top anchorage of the diagonal reinforcement, visible in the photographs in Figures 4c and 4d, occurred in the post-peak regime.

The two connections of beam 3, 3-DL5 and 3-DL6, exhibited a qualitatively similar cracking behavior to beam 2, until near peak resistance. The failure of the weaker end, 3-DL5, occurred with separation of the top concrete cover above the tip of the re-entrant corner crack. The failure of the stronger end, 3-DL6, occurred due to rapid opening of the inclined crack propagating from the inner edge of the support in the dapped end. This was also accompanied by the separation of the top concrete cover.

In the two connections that featured the heaviest amount of reinforcement, 4-DL7 and 4-DL8, the corner crack was relatively small near peak load, with crack displacements in the range of 1 to 2 mm. The inclined shear cracks in the dapped end were visibly wider than the corner crack – see Figs. 4g (left) and 4h (left). The failure of the two connections was much more brittle relative to the other specimens of the test series, as can be seen from the load-deformation plots in Figures 4 and 5. The photograph of specimen 4-DL7 in Figure 4g (middle) shows that the failure occurred in shear due to diagonal crushing of concrete. The crushing occurred between the two inclined cracks in the dapped end, in the region intersected by the main layers of vertical reinforcement. Specimen 4-DL8 also failed in shear by rapid opening of the inclined crack propagating from the edge of the support plate. However, it is important to note that these shear failures occurred after (or near) yielding of the main dapped-end reinforcement.

Figure 6 shows the measurements of the strain gauges attached to the main horizontal, vertical, and diagonal reinforcement. It can be seen that the reinforcement in all connections exhibited significant plastic deformations before failure. As these tests featured no stirrups in the clear shear span, and a considerable amount of reinforcement in the dapped end, this indicates that these connections are more prone to failure along a re-entrant corner crack.

As the failures in the heavily reinforced connections were triggered by the shear cracks in the dapped end, the occurrence and magnitude of these cracks are of interest. An indication of this is given by quantity (DT2-DT4), which represents the sum of vertical displacements of the shear cracks – see green curves in the load-deformation plots of Figure 4. It is evident that, with the exception of the two specimens with the lightest reinforcement (beam 1), the shear cracks occurred at a similar support shear load in the range of $V \approx 300$ kN to 400 kN. The two specimens of beam 1 failed at lower loads, and therefore did not exhibit shear cracks. The sum of the vertical displacements in the shear cracks became similar in magnitude to that of the main corner crack only close to the failure of the connections of beams 2-4.

The horizontal and vertical crack displacements at 50% of the peak load reported in Table 3 provide an indication of the cracking behavior under service conditions. In the connections with the lightest reinforcement, 1-DL1 and 1-DL2, the crack displacements varied in the range of 0.55 mm to 0.72 mm. These values were smaller for the tests with the highest amount of reinforcement, 4-DL7 and 4-DL8, where the crack displacements varied in the range of 0.38 mm to 0.62 mm. While subjected to considerable scatter, the observed trend is that the corner crack width decreased marginally as the reinforcement amount and bar diameters were increased substantially. However, it is important to note that for all specimens the crack displacements were well in excess of typical code provisions for service conditions (0.3-0.4 mm).

The test series with orthogonal reinforcement layout[19] (OL series) displayed qualitatively similar overall behavior as the specimens described in this study. This is not unexpected, as that test series also featured a gradual increase of dapped-end reinforcement in similar quantities. However, a more in-depth analysis of test results is necessary to establish quantitative differences between the diagonal reinforcement layout and the orthogonal reinforcement layout reported in Rajapakse et al. 2022[19].

COMPARISON BETWEEN THE DIAGONAL AND ORTHOGONAL REINFORCEMENT LAYOUTS

As mentioned earlier, the specimens with orthogonal reinforcement layout (OL series) were part of a similar experimental campaign conducted by the authors[19]. The main difference between the DL and OL series was the choice of the reinforcement layout, while the geometry, material properties, and the reinforcement amounts were similar in corresponding tests. In this section, the test results of the DL and OL series are compared and contrasted with respect to ultimate capacity (strength) and crack control.

Strength

Figure 7 illustrates the effect of total amount of dapped-end reinforcement $A_{sh}+A_{sv}+A_{sd}$ on the measured ultimate strength V_u of the DL and OL specimens. The DL series is plotted in continuous lines with filled markers, while the OL specimens are shown as empty markers connected with dotted lines. The plot further distinguishes between the connections with different horizontal-to-vertical reinforcement ratio A_{sh}/A_{sv}, where $A_{sh}/A_{sv}\approx1.5$ and $A_{sh}/A_{sv}\approx0.75$ are denoted by blue and red color, respectively. It can be seen that the increase of strength with increasing amounts of reinforcement was nonlinear for both the DL and OL series, where the rate of increase decreased in the more heavily reinforced specimens. This occurred largely in

part due to the shifting of the failure mode from flexural failures along the re-entrant corner crack to shear failures in the dapped end region of the heavily reinforced specimens. It is interesting to note that there is some nonlinearity in the strength, although the main dapped-end reinforcement yielded prior to the occurrence of shear failures. The shear failures may have prevented the activation of the full hardening range of the reinforcement, in particular in the heavily reinforced connections, where the vertical reinforcement was arranged in layers near the re-entrant corner. Furthermore, the reduction of the lever arms with increasing reinforcement may have also contributed to the nonlinearity in the strength variation.

In the OL series, for the same amount of reinforcement, connections with smaller vertical reinforcement $A_{sh}/A_{sv}\approx1.5$ were slightly stronger than those with $A_{sh}/A_{sv}\approx0.75$. This trend is not as pronounced in the DL series, where only the lightly reinforced specimens were stronger with the $A_{sh}/A_{sv}\approx1.5$ configuration.

More importantly, the difference in strength of the DL and OL specimens are shown by the blue and red shading in Figure 7. It can be seen that, for the same cross-sectional area of reinforcement, the specimens with diagonal reinforcement layouts were considerably stronger than connections with only orthogonal reinforcement in the dapped end. A larger strength increase can be observed in the specimens with $A_{sh}/A_{sv}\approx0.75$ (red color shading). For this configuration, the strength increase was approximately 30% for the smallest and largest values of $A_{sh}+A_{sv}+A_{sd}$. The largest strength increase of ~40% was observed in specimen 3-DL6, which had an intermediate amount of reinforcement area $A_{sh}+A_{sv}+A_{sd}$. This shows that the provision of an alternate load path by the addition of diagonal reinforcement has a significant beneficial impact on the strength of dapped-end connections. However, it must be noted that this increase in strength can only occur if enough displacement capacity is available to simultaneously develop the different strength mechanisms.

Crack control

Figure 8 shows the variation of crack widths and slips at 50% of the peak load (V=0.5V_u) with increasing total area of dapped-end reinforcement. At this load level the reinforcement was still elastic, with the exception of the first stirrup layer of 4-OL7 (see Table 3). The crack widths w and slips s are computed from the DT3 and DT4 measurements at the re-entrant corner of the connection by assuming a crack angle of 45°. In Figure 8, the crack widths are plotted with round markers while square markers denote the slip deformations of the specimen. As before, the DL and OL series are shown by continuous and dotted lines, respectively. The two ratios of orthogonal reinforcement, A_{sh}/A_{sv}≈1.5 and A_{sh}/A_{sv}≈0.75, are denoted by blue and red color curves, respectively.

It can be seen that the DL specimens exhibited relatively smaller crack widths than the OL specimens in tests with high amounts of dapped-end reinforcement. This trend was reversed for small values of A_{sh}+A_{sv}+A_{sd}, where the connections with only orthogonal reinforcement had smaller crack widths at the re-entrant corner. In both DL and OL series, the corner crack widths peaked for intermediate values of A_{sh}+A_{sv}+A_{sd}. This trend was more apparent in the OL tests, while only a marginal variation of crack widths can be seen in the specimens with the diagonal layout. Somewhat surprisingly, the DL specimens with additional vertical reinforcement (A_{sh}/A_{sv}≈0.75 shown in red color) displayed slightly poorer crack control than the corresponding connections with A_{sh}/A_{sv}≈1.5 (shown in blue color). The plot also shows that the slip displacements were considerably smaller compared to the crack widths.

A closer look at crack control under service loads is shown in Figure 9, where the corner crack widths corresponding to a support shear load of up to 50% of the peak resistance (V≤0.5V_u) are plotted. It can be seen that all test specimens from both the DL and OL series displayed excessively wide crack widths under service loads. While the addition of diagonal reinforcement enhanced the crack control, the crack widths were still larger than typical code

limits of 0.3-0.4 mm under service conditions. This shows that the re-entrant corner crack is difficult to control with conventional reinforcement. Excessively wide crack opening of dapped-end connections under service conditions poses significant durability concerns due to penetration of water and other corrosive agents. Therefore, further research needs to be conducted on alternative methods of crack control, such as the use of fiber reinforced concrete[7, 21-22] (FRC), ultra-high performance fiber reinforced concrete (UHPFRC) or prestressing.

CONCLUSIONS

This paper presented experimental research on eight large-scale dapped-end connections featuring diagonal reinforcement layout. The amount of reinforcement and the ratio between the horizontal and vertical reinforcement near the re-entrant corner were varied to capture the main failure modes identified in dapped-end connections. Detailed reporting of local deformations of the re-entrant corner crack, global deformations of the dapped-end connection, and elongation of the main reinforcement was provided with the aid of 56 continuous measurements. These measurements were used in conjunction with crack patterns to provide a comprehensive description of the observed behavior of the test specimens. The test results of this study were compared and contrasted with a similar previous study featuring orthogonal reinforcement layout. The main conclusions of this study are the following:

- The failure of lightly reinforced specimens occurred due to excessive opening of the re-entrant corner crack (flexural failure) and subsequent rupture of the vertical reinforcement. As the reinforcement amount was increased, the failure mode shifted towards a failure with inclined crushing of the concrete in the dapped-end region (shear failure).
- For the same total area of dapped-end reinforcement, test specimens with diagonal reinforcement (DL series) were substantially stronger than the corresponding connections with orthogonal reinforcement layout. This strength increase was more pronounced in the

specimens with a horizontal-to-vertical reinforcement ratio of A_{sh}/A_{sv}≈0.75. For this configuration, the largest strength increase was ~40% in specimens with intermediate reinforcement amount, while the connections with lighter or heavier reinforcement exhibited approximately ~30% increase in strength.

- The provision of diagonal reinforcement resulted in a marginal increase of crack control in heavily reinforced connections. The crack widths at 50% of the peak load were still well in-excess of typical serviceability requirements, highlighting the difficulty of controlling the corner crack with conventional reinforcement. Further research needs to be conducted on alternative methods of crack control, such as the use of fiber reinforced concrete (FRC), ultra-high performance fiber reinforced concrete (UHPFRC) or prestressing.

ACKNOWLEDGMENTS

Financial assistance for this research was provided by the grant BOF 2018: Doctoraatsfonds i.s.m. ULiège: Chathura Rajapakse [Grant Number BOF 2018 – BOF18DOCLI02 – cofin UHasselt-ULiege].

The authors would like to express their gratitude to the Applicatiecentrum Beton en Bouw (structural laboratory) at Hasselt University, where the tests were conducted. The excellent support of Eng. Dan Dragan in conducting the tests, and Dr. Rik Steensels during the design and procurement of the specimens, is greatly appreciated.

REFERENCES

1. Desnerck P, Lees JM, Morley CT (2016) Impact of the reinforcement layout on the load capacity of reinforced concrete half-joints. Engineering Structures, 127, pp.227-239. https://doi.org/10.1016/j.engstruct.2016.08.061
2. Schlaich J, Schäfer K, Jennewein M (1987) Toward a consistent design of structural

concrete. PCI journal 32(3) pp.74-150. https://doi.org/10.15554/pcij.05011987.74.150

3. Schlaich J, Schafer K (1991) Design and detailing of structural concrete using strut-and-tie models. Structural Engineer 69(6) pp.113-125.
4. Cook WD, Mitchell D (1988) Studies of disturbed regions near discontinuities in reinforced concrete members. Structural Journal 85(2) 206-216. DOI: 10.14359/2772
5. Mata-Falcón J, Pallarés L, Miguel PF (2019) Proposal and experimental validation of simplified strut-and-tie models on dapped-end beams. Engineering Structures, 183, 594-609. https://doi.org/10.1016/j.engstruct.2019.01.010.
6. Muttoni A, Fernández Ruiz M, Niketic F, Backes M.-R (2016) Assessment of existing structures based on elastic-plastic stress fields - Modelling of critical details and investigation of the in-plane shear transverse bending interaction, Rapport OFROU, N° 680, pp. 134, Switzerland, October.
7. Mata-Falcón J (2015) Serviceability and Ultimate Behaviour of Dapped-end Beams (In Spanish: Estudio del comportamiento en servicio y rotura de los apoyos a media madera). PhD Dissertation, Universitat Politècnica de València.
8. Nagy-György T, Sas G, Dăescu AC, Barros JA, Stoian V (2012) Experimental and numerical assessment of the effectiveness of FRP-based strengthening configurations for dapped-end RC beams. Engineering structures, 44, pp.291-303. https://doi.org/10.1016/j.engstruct.2012.06.006
9. Desnerck P, Lees JM, Morley CT (2017) The effect of local reinforcing bar reductions and anchorage zone cracking on the load capacity of RC half-joints. Engineering Structures, 152, pp.865-877. https://doi.org/10.1016/j.engstruct.2017.09.021
10. Herzinger R (2008) Stud reinforcement in dapped ends of concrete beams (Vol. 69, No. 05).
11. Zhu RR, Wanichakorn W, Hsu TT, Vogel J (2003) Crack width prediction using

compatibility-aided strut-and-tie model. Structural Journal, 100(4), pp.413-421.

12. Nagrodzka-Godycka K, Piotrkowski P, (2012) Experimental Study of Dapped-End Beams Subjected to Inclined Load. ACI Structural Journal, 109(1). DOI: 10.14359/51683489
13. Moreno-Martínez JY, Meli R (2014) Experimental study on the structural behavior of concrete dapped-end beams. Engineering Structures, 75, pp.152-163. DOI: 10.1016/j.engstruct.2014.05.051
14. Mattock AH, Chan TC (1979) Design and behavior of dapped-end beams. PCI journal, 24(6), pp.28-45.
15. Lu WY, Lin IJ, Hwang SJ, Lin YH (2003) Shear strength of high-strength concrete dapped-end beams. Journal of the Chinese Institute of Engineers, 26(5), pp.671-680.
16. Lu WY, Lin IJ, Yu HW (2012) Behaviour of reinforced concrete dapped-end beams. Magazine of concrete research, 64(9), pp.793-805.
17. Mitchell D, Marchand J, Croteau P, Cook WD (2011) Concorde overpass collapse: structural aspects. Journal of performance of constructed facilities, 25(6), pp.545-553.
18. Mitchell D, Cook WD, Peng T (2010) Importance of reinforcement detailing. Special Publication, 273, pp.1-16.
19. Rajapakse C, Degée H, Mihaylov B (2022) Investigation of shear and flexural failures of dapped-end connections with orthogonal reinforcement. Engineering Structures, 260, p.114233. https://doi.org/10.1016/j.engstruct.2022.114233
20. CEN European Committee for Standardization Eurocode 2. Design of concrete structures Part 1-1: General rules and rules for buildings. Brussels (Belgium): EN 1992-1-1; 2004. p. 225.
21. Mihaylov B, Rajapakse C, Berger PH (2022) Effect of steel fibers on the ultimate flexural behavior of dapped-end connections. Engineering Structures, 259, p.114147.

https://doi.org/10.1016/j.engstruct.2022.114147

22. Fu Z (2004) Use of fibres and headed bars in dapped end beams. MSc Dissertation, McGill University Canada.

TABLES AND FIGURES

List of Tables:

List of Figures:

Table 1– Test variables in the DL and OL series

	Dapped-end reinforcement							f_c (MPa)
	ϕ_h (mm)	A_{sh} (mm^2)	ϕ_v (mm)	A_{sv} (mm^2)	A_{sh}/A_{sv}	ϕ_d (mm)	A_{sd} (mm^2)	
1-DL1	12	226	10	157	1.44	20	314	52.1
1-DL2	12	226	10	314	0.72	20	314	52.1
2-DL3	16	402	8	301	1.36	16	603	51.3
2-DL4	16	402	8	502	0.80	16	603	51.3
3-DL5	20	628	12	452	1.39	16	804	48.1
3-DL6	20	628	12	904	0.70	16	804	48.1
4-DL7	25	982	12	678	1.45	25	1473	46.2
4-DL8	25	982	12	1356	0.72	25	1473	46.2
1-OL1	12	452	8	301	1.50	-	-	56.8
1-OL2	12	452	8	603	0.75	-	-	56.8
2-OL3	16	804	10	628	1.28	-	-	56.4
2-OL4	16	804	10	1099	0.73	-	-	56.4
3-OL5	20	1256	12	904	1.39	-	-	49.6
3-OL6	20	1256	12	1808	0.70	-	-	49.6
4-OL7	25	1964	12	1356	1.45	-	-	52.0
4-OL8	25	1964	12	2712	0.72	-	-	52.0

ϕ_h=diameter of dapped-end horizontal reinforcement, A_{sh}=total area of dapped-end horizontal reinforcement, ϕ_v=diameter of dapped-end vertical reinforcement, A_{sv}=total area of dapped-end vertical reinforcement, ϕ_d=diameter of diagonal reinforcement, A_{sd}=total area of diagonal reinforcement, f_c=compressive strength of concrete. Shaded portion of the table corresponding to the OL series is reported as provided in Rajapakse et al. 2022[19].

Table 2– Mechanical properties of reinforcement

ϕ (mm)	f_y (MPa)	f_u (MPa)	ε_y (‰)	ε_u (%)	E_s (GPa)
8	521	643	2.97	9.82	175
10	509	643	2.72	11.32	187
12	537	634	2.65	12.04	203
16	599	703	3.03	9.27	198
20	598	694	2.93	9.00	204
25	540	647	2.64	9.98	204
32	615	664	3.24	11.36	190

ϕ=bar diameter, f_y=yield strength, f_u=ultimate strength, ε_y=yield strain, ε_u=ultimate strain, E_s=modulus of elasticity

Table 3– Main test results from the DL and OL series

Test	First cracking (kN)	50% of peak load		First yield of dapped-end reinforcement								Peak load			Remarks
		w_h (mm)	w_v (mm)	Sequence of yielding	V_y (kN)	V_y/V_u (%)	ε_{sh} (‰)	ε_{sv} (‰)	ε_{sd} (‰)	w_h (mm)	w_v (mm)	V_u (kN)	w_h (mm)	w_v (mm)	
1-DL1	40	0.55	0.55	V-H-D	165	64	2.37	2.72	2.23	0.85	0.85	257	6.4	6.4	Flexural failure with rupture of the dapped-end vertical reinforcement
1-DL2	44	0.72	0.72	V-D-H	184	62	2.24	2.72	2.48	0.97	0.97	299	9.0	9.0	Flexural failure with rupture of the dapped-end vertical reinforcement
2-DL3	47	0.56	0.71	D-V-H	347	67	2.46	2.74	3.03	0.74	0.99	524	7.3	7.3	Combined failure with rupture of main vertical reinforcement & wide shear cracks
2-DL4	28	0.56	0.93	V-D-H	349	62	2.58	2.97	2.76	0.60	1.13	559	6.7	7.8	Combined failure with rupture of main vertical reinforcement & wide shear cracks
3-DL5	20	0.62	0.35	D-V-H	527	67	2.23	2.40	3.03	0.81	0.42	782	7.7	1.0	Shear failure after reaching flexural plateau, with spalling of the top cover
3-DL6	53	0.96	0.63	D-V-H	596	68	2.13	2.39	3.03	1.26	0.87	876	13.1	4.5	Shear failure after reaching flexural plateau, with spalling of the top cover
4-DL7	16	0.38	0.62	V-D-H	678	75	1.86	2.65	2.33	0.56	0.95	903	1.3	1.6	Shear failure after reaching the flexural plateau
4-DL8	24	0.42	0.48	D-V-H	804	74	1.88	2.10	2.64	0.68	0.79	1088	1.1	1.3	Shear failure after reaching the flexural plateau
1-OL1	75	0.30	0.34	V-H	151	62	2.47	2.96	-	0.45	0.55	245	4.9	6.5	Flexural failure with rupture of the dapped-end vertical reinforcement
1-OL2	80	0.39	0.53	H-V	161	57	2.65	2.02	-	0.50	0.64	283	3.1	2.6	Shear failure after reaching the flexural plateau
2-OL3	86	0.48	0.81	V-H	266	56	2.16	2.72	-	0.56	1.06	472	10	10	Flexural failure with rupture of the dapped-end vertical reinforcement
2-OL4	65	0.70	0.97	V-H	319	57	2.43	2.72	-	0.82	1.11	555	11	12	Shear failure after reaching flexural plateau, with spalling of the top cover
3-OL5	49	1.36	1.20	V-H	325	52	1.76	2.65	-	1.56	1.29	628	7.2	4.9	Shear failure after reaching flexural plateau, with spalling of the top cover
3-OL6	49	0.58	0.88	V-H	506	70	2.24	2.65	-	0.87	1.25	728	8.6	6.0	Shear failure after reaching the flexural plateau
4-OL7	51	0.93	1.12	V-H	396	46	1.66	2.65	-	0.90	1.12	868	7.4	6.2	Shear failure after reaching the flexural plateau
4-OL8	43	0.89	0.79	V-H	564	57	2.25	2.65	-	1.12	0.99	995	4.6	3.1	Shear failure after reaching the flexural plateau

w_h=horizontal displacement component of the re-entrant corner crack measured by DT 3, w_v=vertical displacement component of the re-entrant corner crack measured by DT 4, V_y= support shear load at first yield of dapped-end reinforcement, ε_{sh}=strain of dapped-end horizontal reinforcement, ε_{sv}=strain of first layer of dapped-end vertical reinforcement, V_u= support shear load at peak load, *H*=dapped-end horizontal reinforcement, *V*=first layer of dapped-end vertical reinforcement. Shaded portion of the table corresponding to the OL series is reported as provided in Rajapakse et al. 2022[19].

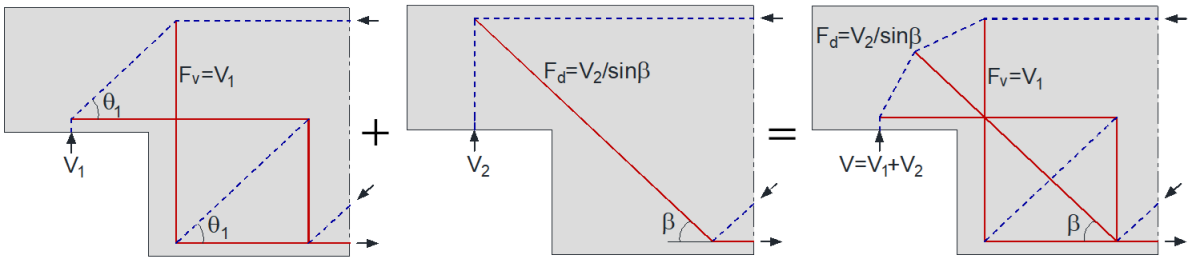

Fig. 1 – Strut-and-tie model for dapped-end connections with diagonal reinforcement: Schlaich et al. 1991[3]

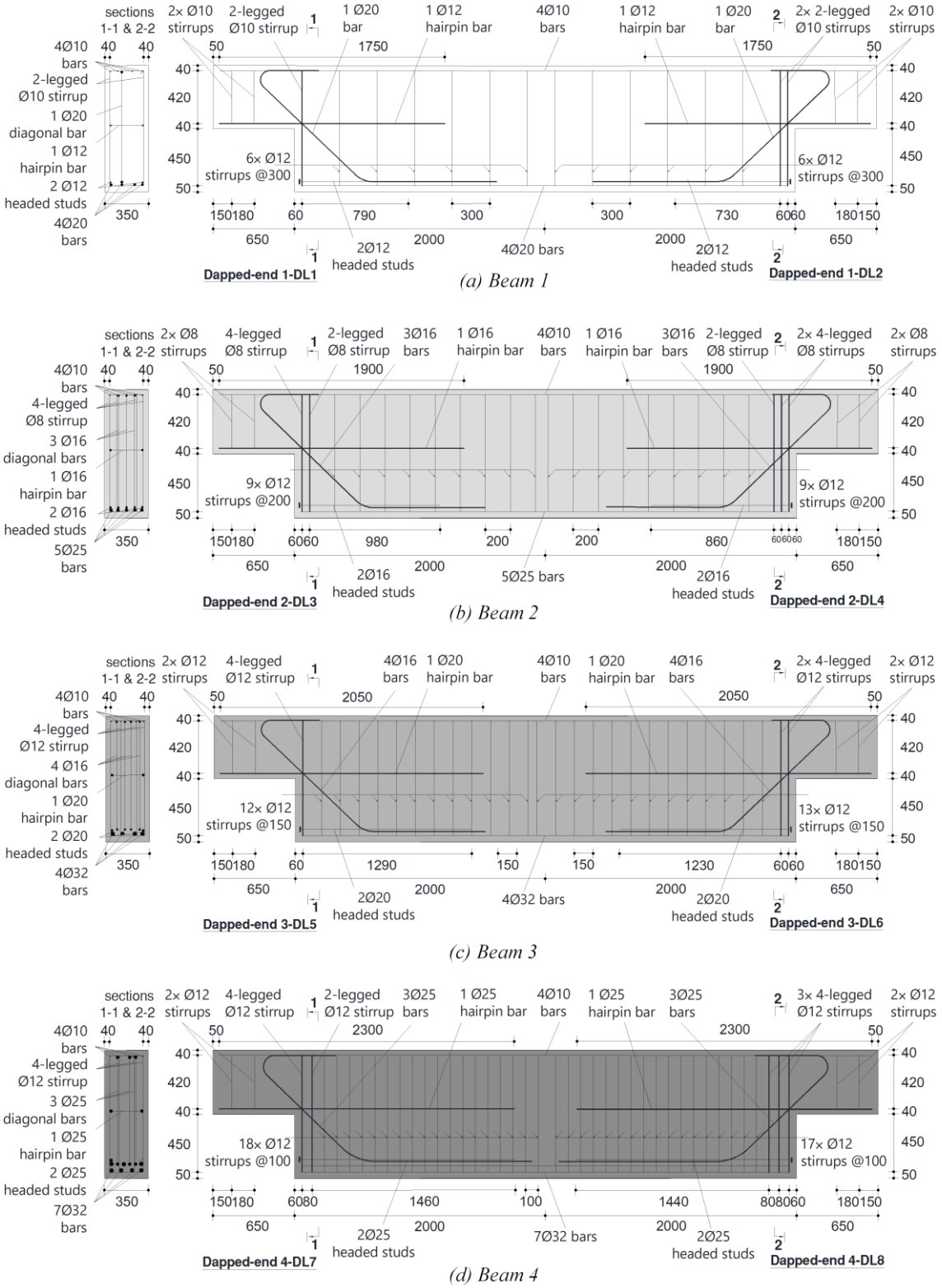

Fig. 2 – Test specimens (dimensions in mm)

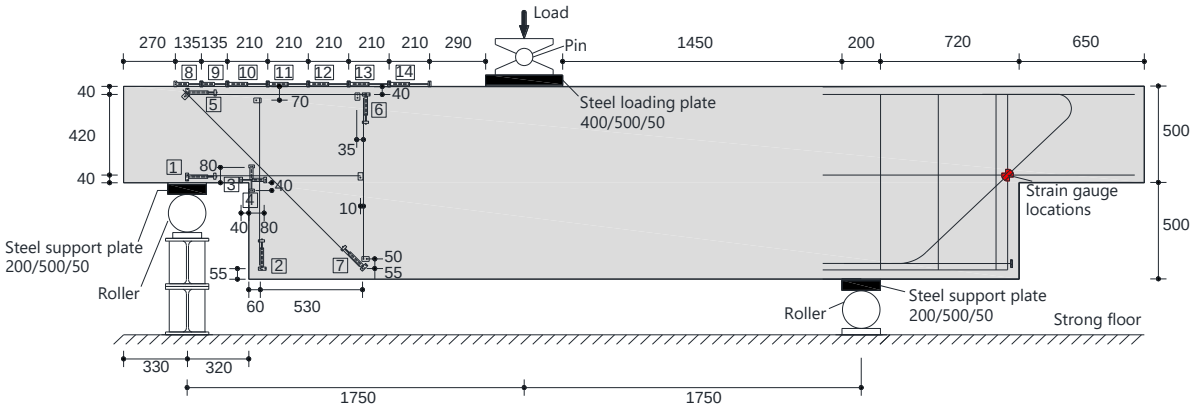

Fig. 3 – Test setup and instrumentation (dimensions in mm)

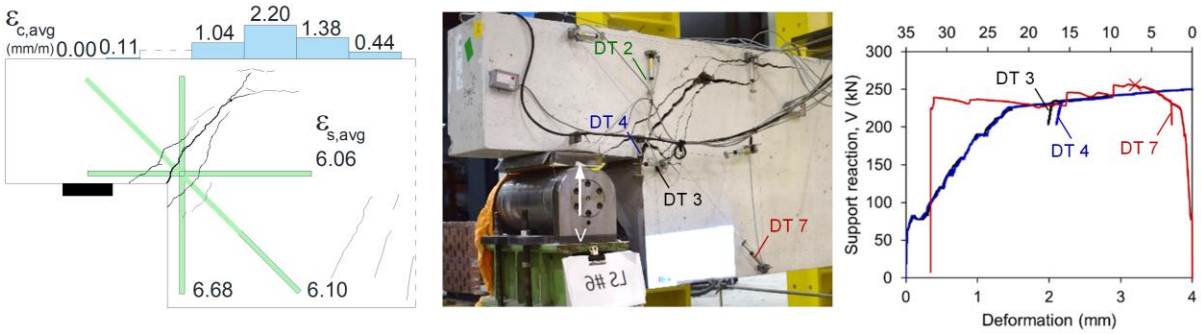

(a) Beam 1-DL1: left – crack pattern near peak load (256 kN, corresponds to the X mark in the figure on the right), middle – after failure, right – support reaction vs. crack components at the re-entrant corner

(b) Beam 1-DL2: left – crack pattern near peak load (298 kN), middle – after failure, right – support reaction vs. crack components at the re-entrant corner

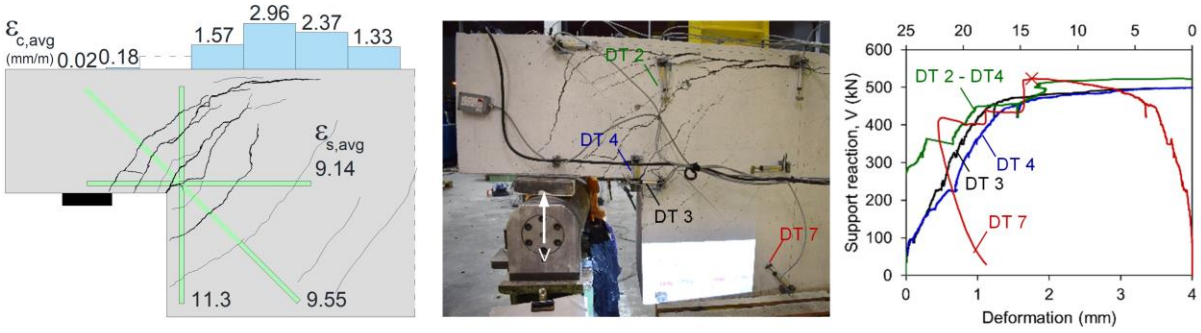

(c) Beam 2-DL3: left – crack pattern near peak load (523 kN), middle – after failure, right – support reaction vs. crack components at the re-entrant corner

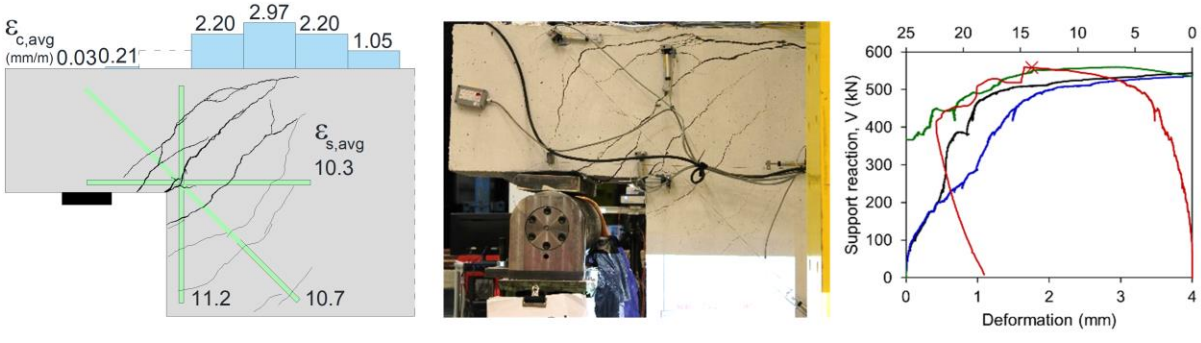

(d) Beam 2-DL4: left – crack pattern near peak load (559 kN), middle – after failure, right – support reaction vs. crack components at the re-entrant corner

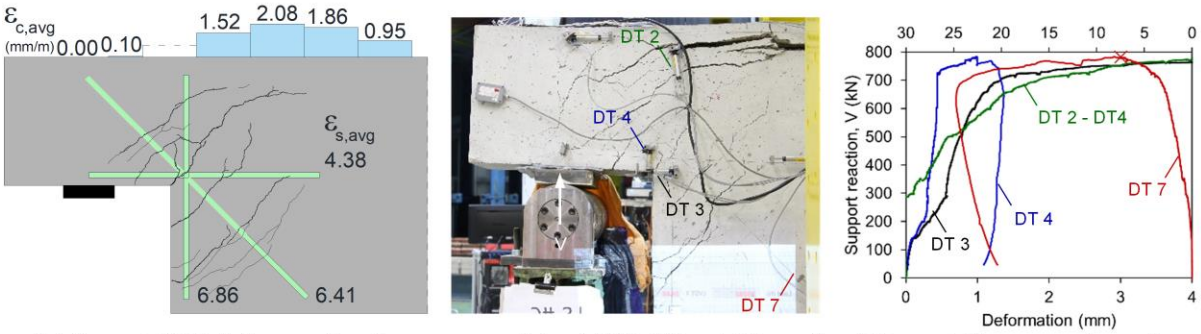

(e) Beam 3-DL5: left – crack pattern near peak load (782 kN), middle – after failure, right – support reaction vs. crack components at the re-entrant corner

(f) Beam 3-DL6: left – crack pattern near peak load (875 kN), middle – after failure, right – support reaction vs. crack components at the re-entrant corner

(g) Beam 4-DL7: left – crack pattern near peak load (900 kN), middle – after failure, right – support reaction vs. crack components at the re-entrant corner

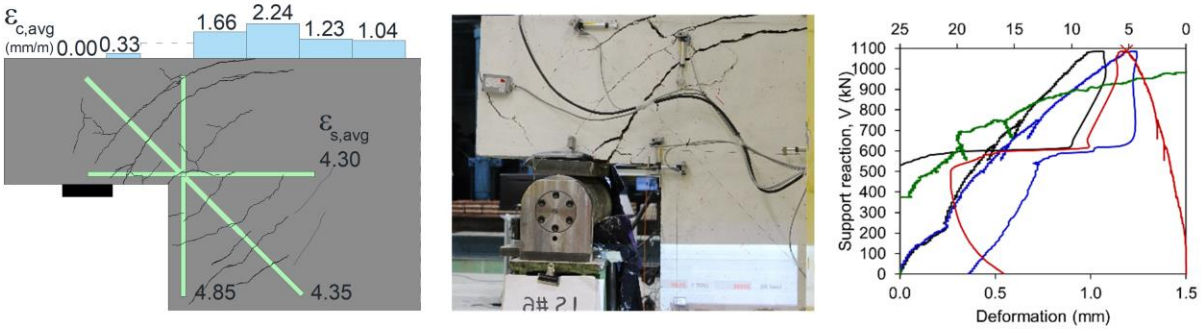

(h) Beam 4-DL8: left – crack pattern near peak load (1088 kN), middle – after failure, right – support reaction vs. crack components at the re-entrant corner

Fig. 4 – Overview of test results

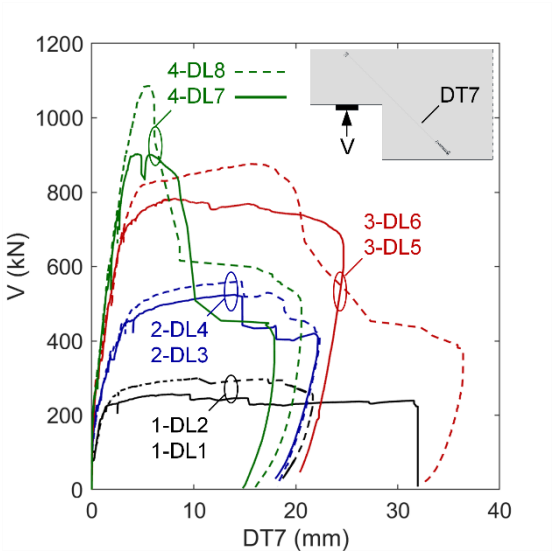

Fig. 5 – Strength and ductility of the test specimens

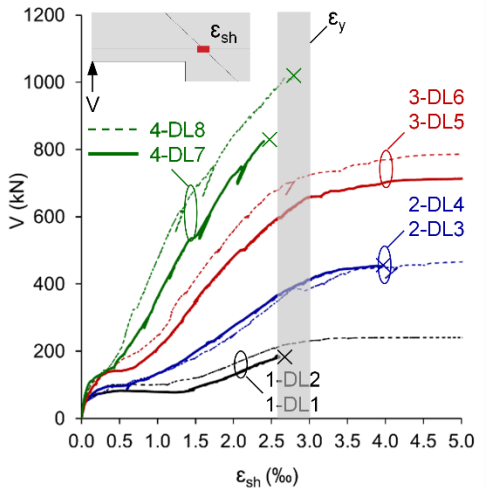

(a) Dapped-end horizontal reinforcement (X mark indicates strain gauge malfunction)

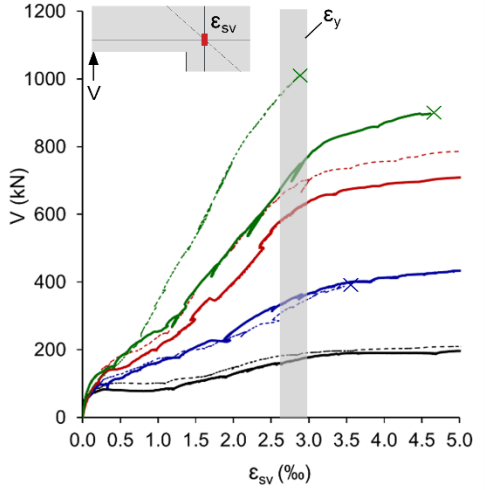

(b) First layer of dapped-end vertical reinforcement

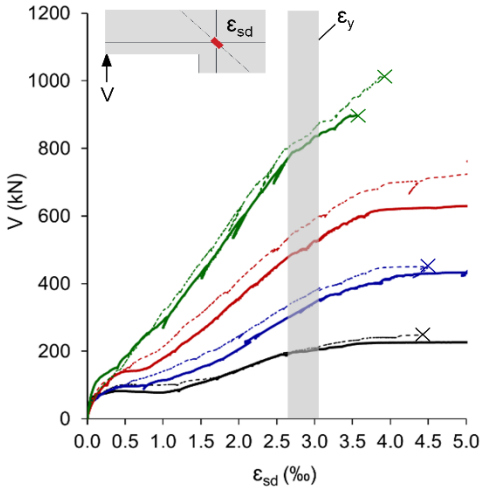

(c) Diagonal reinforcement

Fig. 6 – Measured strains of main dapped-end reinforcement

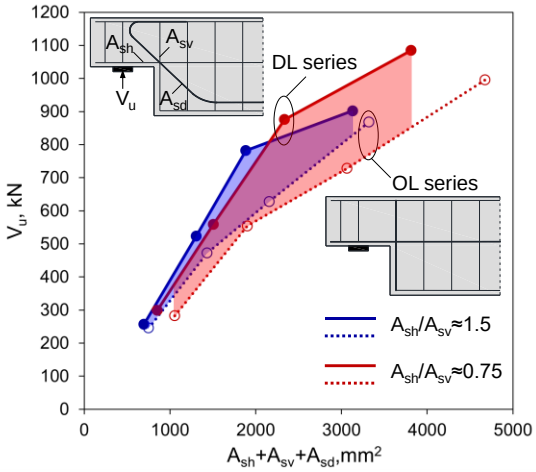

Fig. 7 – Effect of total amount of dapped-end reinforcement on the measured strength

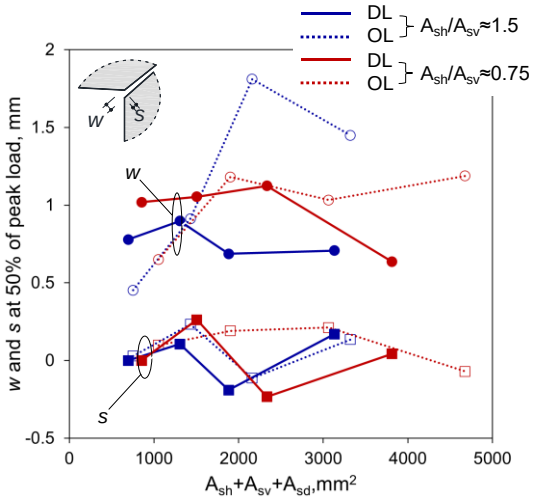

Fig. 8 – Displacements in the re-entrant corner crack at 50% of the peak load

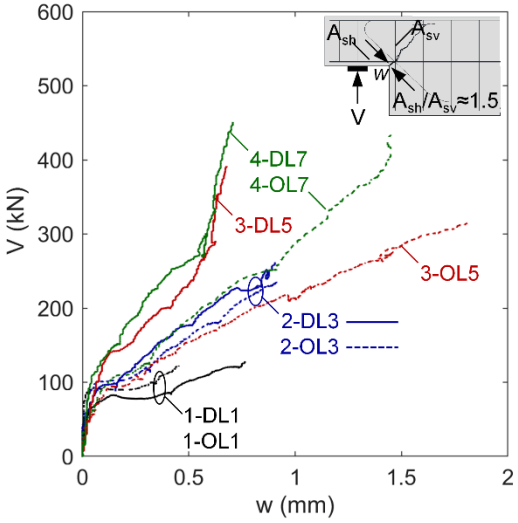

(a) A_{sh}/A_{sv}≈1.5 configuration

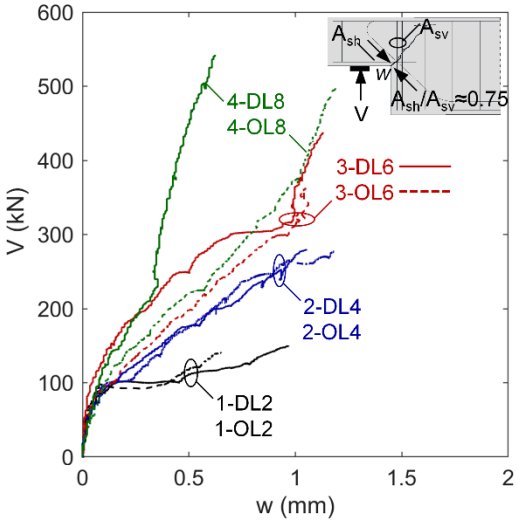

(b) A_{sh}/A_{sv}≈0.75 configuration

Fig. 9 – Crack widths at the re-entrant corner under service loads (for $V \leq V_u$)